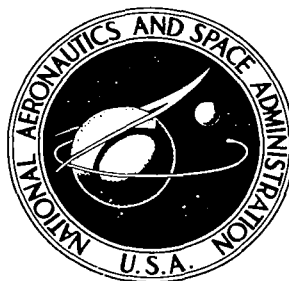


NASA TECHNICAL NOTE

NASA TN D-6466



NASA TN D-6466

C.1

0133292



TECH LIBRARY KAFB, NM

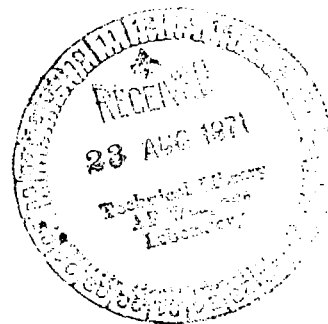
LOAN COPY: RETI
AFWL (DOGL
KIRTLAND AFB,

GRAPHITE MINORITY CARRIERS, FROM
TRANSPORT MEASUREMENTS TO 10 TESLAS

by John A. Woollam

Lewis Research Center

Cleveland, Ohio 44135





0133292

1. Report No. NASA TN D-6466		2. Government Accession No.		3. Recipient's Catalog No.	
4. Title and Subtitle GRAPHITE MINORITY CARRIERS, FROM TRANSPORT MEASUREMENTS TO 10 TESLAS				5. Report Date August 1971	
				6. Performing Organization Code	
7. Author(s) John A. Woollam				8. Performing Organization Report No. E-6334	
9. Performing Organization Name and Address Lewis Research Center National Aeronautics and Space Administration Cleveland, Ohio 44135				10. Work Unit No. 129-02	
				11. Contract or Grant No.	
				13. Type of Report and Period Covered Technical Note	
12. Sponsoring Agency Name and Address National Aeronautics and Space Administration Washington, D.C. 20546				14. Sponsoring Agency Code	
15. Supplementary Notes					
16. Abstract Study of quantum oscillations in the Hall effect and thermoelectric-power indicates that there are at least two sets of minority carriers in graphite. Natural single crystals and pyrolytic graphite have the same minority Fermi surface sections, and their possible locations in the Brillouin zone are discussed. Under the assumption that the band parameter γ_0 is 2.85 eV, the band parameter Δ is estimated to be +0.008 eV.					
17. Key Words (Suggested by Author(s)) Galvanomagnetic effects Graphite Thermomagnetic effects Minority carriers Fermi surfaces Band structure Oscillatory Hall effect				18. Distribution Statement Unclassified - unlimited	
19. Security Classif. (of this report) Unclassified		20. Security Classif. (of this page) Unclassified		21. No. of Pages 16	
				22. Price* \$3.00	

GRAPHITE MINORITY CARRIERS, FROM TRANSPORT MEASUREMENTS TO 10 TESLAS

by John A. Woollam
Lewis Research Center

SUMMARY

The quantum oscillations in the Hall effect and thermoelectric power are studied in two samples of pressure-annealed pyrolytic graphite. Only the oscillations originating from minority Fermi surface carriers are discussed. Frequencies of the de Haas - van Alphen type are measured over a wide range of angles between the magnetic field and the C axis of the Brillouin zone. The major conclusions are (1) there are at least two minority carriers in graphite, (2) pyrolytic and natural single crystals have the same minority Fermi surface sections, (3) both minority carriers observed by quantum effects very likely originate from the corners of the Brillouin zone near the H points, and (4) under the assumption that the band parameter γ_0 is 2.85 eV we estimate that the band parameter Δ is +0.008 eV.

INTRODUCTION

Crystalline, hexagonal graphite has two sets of Fermi surfaces. There are two large, or "majority," sections, one electron and one hole, which are fairly well understood (refs. 1 to 3). There are also at least two very small, or "minority," sections. The nature (electron or hole) and location (in the Brillouin zone) of these carriers is not well understood.

The first evidence for the existence of minority carriers was from cyclotron resonance experiments (refs. 4 and 5), and from Hall effect studies (refs. 6 and 7). One of the first detailed studies of minority carriers was by Soule on natural single crystals using the de Haas - van Alphen (DHVA) effect (ref. 8). Later Williamson, Foner, and Dresselhaus (ref. 3) reported minority carrier de Haas - van Alphen frequencies in both pyrolytic and natural single-crystal graphite. Williamson's pyrolytic, and Soule's single-crystal results were very different from each other.

Both Soule (ref. 8), and Williamson, Foner, and Dresselhaus (ref. 3) studied the dependence of DHVA period on angle between the C axis (symbols are defined in the appendix) and the magnetic field H. In natural single crystals Soule found a period of 1.35 tesla^{-1} ($1\text{T} = 10 \text{ kG}$) for H parallel to C and 0.15 tesla^{-1} for H perpendicular to C. Their periods are plotted against angle in figure 1. The ratio of the two is the anisotropy ratio and is equal to 9. The observation of these oscillations for H perpendicular to C suggested to Soule that the Fermi surface was closed. Anderson, O'Sullivan, Schirber, and Soule (ref. 9) have confirmed the results of Soule on natural single crystals for H parallel to C.

In pyrolytic graphite Williamson found quite different results. For H parallel to C the period was approximately 2.94 tesla^{-1} , as shown in figure 1. (The results reported in ref. 2 were wrong because of magnet calibration error, which was later corrected.) Williamson, Foner, and Dresselhaus were only able to observe oscillations out to about 70° from C in their pyrolytic sample. It was not at all certain if this was the same carrier as that studied by Soule in a natural single crystal.

Flood (refs. 10 and 11) recently found a minority period of $0.85 \pm 0.20 \text{ tesla}^{-1}$ (see fig. 1) for H parallel to C on a pyrolytic sample (sample PG-1) having 300 to 4.2 K resistance ratio of about unity. Results on PG-1 to PG-6 are reported elsewhere (refs. 1, 2, and 12). This period is closer to Soule's single-crystal value (dashed line, fig. 1) than that found in Williamson's pyrolytic sample.

Since Soule's work (ref. 6) on single crystals, the very low magnetic field (nonquantum oscillatory region) Hall effect has been used by Spain to detect the presence of minority carriers in pyrolytic graphite (ref. 13). Spain observes both minority electrons and holes, depending on temperature.

In the present report, minority carriers are studied by observing the oscillations (in magnetic field) in the Hall voltage and thermopower. Two samples of pressure-annealed pyrolytic graphite are studied. The periods are measured as a function of the angle θ between the magnetic field H and the C axis, where $0 \leq \theta \leq 87^\circ$. These results are compared with all previous data, and a remarkable similarity between natural single-crystal and pyrolytic graphite results is demonstrated. The location of minority carriers in the Brillouin zone is discussed, and an estimate of the band parameter Δ is made.

THEORY

Quantum Oscillations

The theory for quantum oscillations is well established and is discussed in many standard texts (ref. 14). The effect results from the quantization of electron orbital motion in the presence of an applied magnetic field. The resultant energy levels (Landau levels) depend on field strength. As the magnetic-field strength changes, the Landau levels move through Fermi surface boundaries. The familiar oscillations (DHVA) in magnetic susceptibility result. The effects of the Landau level crossings of the Fermi energy on the Hall effect and thermoelectric power are not as frequently studied. (See, however, ref. 1). Yet, these effects are useful since their amplitudes are frequently sensitive to features of the Fermi surface, while the amplitudes of other oscillating effects are not. Other reasons for studying transport effects are discussed in reference 1. All effects yield the same period P . It is often desirable to express the results as a frequency F , where

$$F = \frac{1}{P} \quad (1)$$

The frequency F is proportional to the extremal cross-sectional area of the Fermi surface perpendicular to the magnetic-field direction.

The theory for quantum oscillations in the Hall effect can be found in reference 15. Thermopower quantum effects are discussed in reference 1.

Band Structure of Graphite

Majority carriers. - A frequently used energy band structure of graphite was calculated by Slonczewski and Weiss (ref. 16) and parameterized by McClure (ref. 17). Results of the calculation show that energy levels can be determined when the following parameters in the band structure theory are found experimentally:

$$\gamma_0 = 2.85 \text{ eV} \quad (2a)$$

$$\gamma_1 = 0.31 \text{ eV} \quad (2b)$$

$$\gamma_2 = -0.0185 \text{ eV} \quad (2c)$$

$$\gamma_3 = 0.29 \text{ eV} \quad (2d)$$

$$\gamma_4 = 0.18 \text{ eV} \quad (2e)$$

$$\gamma_5 = -0.0183 \text{ eV} \quad (2f)$$

$$\Delta = 0.025 \text{ eV} \quad (2g)$$

The values quoted have been principally determined from circularly polarized magnetoreflexion and the de Haas - van Alphen effect measurements (refs. 3 and 18).

The γ 's determine the carrier effective mass, the extremal areas, and the DHVA period anisotropy ratios. Conversely, the γ 's are partially determined from experimental measurements of these quantities.

Minority carriers. - There have been several suggestions as to the location of minority carriers in the Brillouin zone. The majority carrier Fermi surfaces are shown in figure 2, along with possible minority carriers. The hexagonal "pill box" Brillouin zone of graphite is shown with Fermi surfaces drawn on only one of the vertical edges. These surfaces would actually be present on all edges. Noziere (ref. 19) suggested that minority carriers could be formed by strong trigonal warping of the majority electron surfaces. This is the origin of the three minority electron sections pictured in figure 2. However, strong trigonal warping implies a large value of γ_3 . In order to produce the separate minority carriers shown in figure 2 the band parameter γ_3 would have to be at least three times larger than the value listed in equation (2d). Therefore, the existence of these sections is doubtful.

Williamson, Foner, and Dresselhaus (ref. 3) suggested that the surfaces near the points H (fig. 2) were the origin of their observations (large period in fig. 1). At H there are two extremal areas which could give rise to quantum oscillations denoted by α and β in figure 2. The smaller area, β , shown as an ellipsoid would have the larger period. The outer section α is actually part of the majority carrier holes, but the extremal area near the edge of the zone gives rise to minority carrier effects. Both sections are holes. The cross-sectional areas can be estimated from the Slonczewski-Weiss band model (ref. 16) as follows:

$$A_m = 4\pi E_F \frac{(E_F - \Delta)}{3a_0^2 \gamma_0^2} \quad (3)$$

where E_F is the Fermi energy, a_0 is the lattice spacing in the plane perpendicular to C, A_m is the extremal area perpendicular to the C axis with no spin-orbit interaction.

Spin-orbit coupling produces two quantum oscillation frequencies by changing equation (3) by an amount

$$\frac{\delta A}{A} (H \parallel c) \simeq \frac{\pm 2 \Delta}{E_F(E_F - \Delta)} \quad (4)$$

EXPERIMENTAL PROCEDURE

The samples (provided by Dr. A. W. Moore) used in the present experiments were made by stress annealing pyrolytic graphite. These samples are polycrystalline but with individual grains aligned, with C axes having a 2° half-width about a common direction. The ratio of 300 to 4 K resistance was 1.5 for PG-3 and approximately 4 for PG-6.

The Hall effect measurements were made on PG-6 after shaping the sample with a sand erosion cutter into a long bar with small tabs on the sides for leads. Constant current was provided in the basal plane, and voltage was measured with a nanovolt amplifier, as illustrated in figure 3.

The adiabatic thermopower (ref. 1) was measured with constant heat input to one end of the sample. A similar tab arrangement was used for attaching leads. Voltages were measured having a typical noise level of 0.1 microvolt.

Measurements were made in two magnets. The first magnet used was a superconducting split pair, providing 4.0 teslas (1 T = 10 kG) in a transverse configuration. The second magnet was a superconducting solenoid having a maximum field of 10.5 teslas. An insert Dewar for this magnet permitted pumping helium to 1.0 K in a 0.054-meter- (2.5-in. -) diameter test region. Fields were measured in the solenoid by using a magnetoresistor calibrated with nuclear magnetic resonance. In the split pair magnet, the field was measured by integrating the induced voltage produced by the sweeping field.

RESULTS

Thermopower in Sample PG-3

In figure 4 the thermopower in sample PG-3 is plotted as a function of magnetic field at 1.2 K for $H \perp C$ from the C axis. The majority carrier oscillations are superimposed on the lower frequency minority carrier oscillations. The majority carrier thermopower effects are discussed extensively in references 1 and 2. In figure 4 the minority extrema are marked by arrows. The minority carrier oscillations could easily be followed to large angles between the magnetic field and the C axis because

their amplitudes do not die out as rapidly with angle as do the majority carrier oscillations. For example, at $\theta = 75^\circ$, there are 10 minority carrier extrema observable below 2.0 teslas (20 kG) but only two or three majority carrier oscillations. The thermopower minority DHVA periods were measured out to $\theta = 80^\circ$, and these are plotted in figure 1. Our pyrolytic periods are, within experimental error, the same as Soule's natural single-crystal periods.

Williamson's results on a pyrolytic sample are plotted in figure 1. At $\theta = 0$ he gets $F = 0.34 \pm 0.015$ tesla or a period of approximately $3.0 \pm 0.1 \text{ tesla}^{-1}$. As is visible from figure 1, these results are quite different from the results on natural single crystals and the pyrolytic results presented in this report.

Hall Effect in Sample PG-6

The Hall effect ρ_{yx} in a second sample, PG-6, was studied extensively for minority carrier effects. It is also a pressure-annealed pyrolytic sample having a resistance ratio R_{300K} to $R_{4.2K}$ of 3.5. In this sample the minority carrier effects could be seen to $\theta = 87^\circ$. The magnetoresistance ρ_{yy} anisotropy was used to locate accurately the angles close to $\theta = 90^\circ$. In figure 5, the magnetoresistance is plotted as a function of angle at a field of 10.2 teslas (102 kG). At $\theta = 90^\circ$ there is a sharp minimum which was used to locate $\theta = 90^\circ$ to within $\pm 1/4^\circ$.

Examples of the minority oscillations in the Hall resistance as a function of magnetic field are shown in figure 6 for $\theta = 77^\circ$. At low fields the minority carrier oscillations dominated. The majority carrier oscillations were not visible below about 4 teslas. For θ greater than 80° there were no majority carrier oscillations present in fields to 10 teslas.

The Hall effect results on PG-6 are shown in figure 1. For θ between 80° and 90° the quantum oscillation results as a function of angle are better seen as plots of frequency than as plots of period. In figure 7 the Hall frequencies in PG-6 are plotted as a function of angle. If the originating Fermi surface were a cylinder, then the frequency would be

$$F = F(0) \sec \theta \quad (5)$$

where $F(0)$ was measured at $\theta = 0$ to be 0.9 ± 0.1 tesla. Equation (5) is plotted in figure 7 assuming $F(0) = 0.6$ tesla, $F(0) = 1.2$ teslas, and $F(0) = 0.9$ tesla. The value $F(0) = 0.9$ tesla appears to fit the data best. Thus the data can be fitted, within experimental error, to the equation

$$F = 0.9 \sec \theta \quad (6)$$

for θ between 0° and 87° . This suggests that the Fermi surface is an extremely elongated ellipsoid. The frequency ratio is

$$\frac{F(\theta = 87^\circ)}{F(\theta = 0^\circ)} = 13.5 \quad (7)$$

and it increases rapidly with increasing θ .

INTERPRETATION AND DISCUSSION

In figure 1 there is close agreement between the data from two independent natural single crystals and two independent pyrolytic samples. A third pyrolytic (Flood's) gives near agreement. This indicates that both pyrolytic and natural single crystals have the same minority Fermi surface pocket of carriers. Since the band structure depends sensitively on minority carriers, this suggests that the two band structures are very nearly the same.

That Williamson's results in a pyrolytic sample are so different indicates that (1) there are two distinct pockets of minority carriers, and he is observing the other one, or (2) his pyrolytic sample has dissolved impurities in it. There is evidence for conclusion (1) in the results of Soule (ref. 8) and in some unpublished single-crystal results of Williamson, where both authors report seeing two de Haas - van Alphen frequencies. Conclusion (2) is possible because a minority pocket size will change rapidly with doping, as shown by Soule (ref. 6). Soule's doping by boron reduced the period, whereas the period would have to be increased to explain Williamson's results.

The three electron carriers shown opposite the K point in figure 2 are probably not being observed in the present experiments for the following reasons: The extreme anisotropy of DHVA frequencies with angle observed in PG-6 is probably too large. It would take $\gamma_3 = 0.9$ eV (refs. 8 and 19), which is three times larger than magnetoreflexion results (ref. 18) indicate for this parameter.

The other possible location of minority carriers is near the points H in the Brillouin zone (see fig. 2). With spin-orbit coupling included, there will be two minority sections near H as shown and discussed earlier. Since the majority carriers near this point are hole carriers, the minority carriers will both be holes. In fact, one of the minority sections is a narrow part of the majority surface. Being an extremal cross section, it will give rise to a low-frequency oscillation. This section (call it α) will be extremely anisotropic in cross-sectional area. For $\theta = 90^\circ$ this will have a frequency of approximately twice the majority hole frequency, assuming no magnetic breakdown. From Soule, McClure, and Smith's (ref. 20) majority carrier data, this frequency will

be 133 teslas. From our results on PG-6, the frequency for $\theta = 0$ is 0.9 tesla. Thus, the anisotropy ratio for the α minority carrier is expected to be approximately

$$\frac{F(\theta = 90^\circ)}{F(\theta = 0^\circ)} = 148$$

with no magnetic breakdown, or 74 with breakdown present.

As discussed by Williamson, Foner, and Dresselhaus (ref. 3) the expected anisotropy ratio for the small, ellipsoid (β) is expected to be 2.3. Since we find that the ratio is greater than 13 and still increasing with angle for PG-6, it is concluded that we have observed the α minority carrier.

We conclude that Williamson's very low frequency (greater period) observations in pyrolytic graphite originated from the β surface. His observed anisotropy ratio of 1.9 ± 0.5 is close to that predicted for this section. Williamson's de Haas - van Alphen frequency was also small and indicated a smaller cross-sectional area than the α section.

The expected cross-sectional area of the minority carriers near the H points can be estimated by using equation (3). Using the parameters of equation (2) the area is $7.3 \times 10^{15} \text{ meter}^{-2}$, which corresponds to a period of 1.3 tesla^{-1} . This is within a factor of 2 of the observed values, which is a reasonable proportion since the calculation is sensitive to the value of Δ used. There have been a wide range of estimates for Δ (see ref. 3, for example).

McClure and Yafet (ref. 21) estimated the spin-orbit coupling constant to be $\lambda \sim 2 \times 10^{-4} \text{ eV}$, and recent spin splitting data (refs. 12 and 22) show that λ is less than 10^{-3} eV . (McClure has made a detailed analysis (including γ_3 effects) of the data of ref. 9 and also concludes that λ is less than 10^{-3} eV .) From equation (4) the shifts in frequency are less than 1 percent for $\lambda = 10^{-3} \text{ eV}$. Thus, the factor of 2 separation in periods shown in figure 1 is not due to spin-orbit coupling alone. Tsukada and Uemura (unpublished data) have shown that stacking faults in the crystal could have effects similar to, but much larger than, spin-orbit coupling. The effect would be to separate the frequencies and produce two independent branches as shown in figure 1.

The lower period branch shown in figure 1 was the dominant carrier seen by Soule, and his data overlap the PG-3 and PG-6 data in both magnitude and angular dependence out to $\theta = 80^\circ$. This is most likely the α section. His second frequency is roughly the same as observed by Williamson (see fig. 1) and would be from the β section. The only unexplained feature of this assignment is the anisotropy ratio. In PG-6 the anisotropy ratio was greater than 13 at $\theta = 87^\circ$ and could become very large at $\theta = 90^\circ$. Soule's ratio was 9 at $\theta = 90^\circ$, and this ratio is much smaller than expected for the α surface. This is the only discrepancy we can find in the assignment of the two period

branches of figure 2 to the α and β sections. Soule has pointed out (unpublished data) that the discrepancy could be explained by a very small angle between the rotation planes in which θ is measured.

With the α and β assignment then, the frequency which would result if there were no stacking faults or spin-orbit coupling would be 0.467 tesla. Two estimates of Δ can be made from equation (3): If $\gamma_0 = 2.85$ eV (ref. 18), then $\Delta = +0.008$ eV. If $\gamma_0 = 3.18$ eV (ref. 3), then $\Delta = +0.016$ eV.

CONCLUSIONS

Quantum oscillation frequencies were studied by using the thermoelectric power and Hall effect for two independent samples of pressure-annealed pyrolytic graphite. These frequencies were obtained over a wide range of angles between the magnetic field and the C axis. From the present experiments and from the results of previous workers, there are four major conclusions:

1. There are at least two minority carrier sections of the Fermi surface in graphite.
2. Pyrolytic and single-crystal graphite have the same minority Fermi surface sections.
3. Both minority sections very likely originate from the corners of the Brillouin zone, near the H points.
4. The band parameter Δ is +0.008 eV if we assume the band parameter γ_0 is 2.85 eV.

Lewis Research Center,
National Aeronautics and Space Administration,
Cleveland, Ohio, May 28, 1971,
129-02.

APPENDIX - SYMBOLS

A_m	extremal cross-sectional area of minority carrier Fermi surface
C	axis parallel to hexagonal (0001) axis of Brillouin zone
c	speed of light
E_F	Fermi energy
e	electronic charge
F	de Haas - van Alphen frequency, $1/P$
δF	change in de Haas - van Alphen frequency
F_α	frequency of α surface
F_β	frequency of β surface
H	magnetic field
H, K	points in Brillouin zone
\hbar	Planck's constant/ 2π
m	free electron mass
P	de Haas - van Alphen period, $1/F$
P_α, P_β	period of α and β sections
α	minority section with larger frequency located at H points of Brillouin zone
β	minority section with lower frequency located at H points of Brillouin zone
$\gamma_0, \gamma_1, \gamma_2, \gamma_3, \gamma_4, \gamma_5, \Delta, a_0$	parameters of band structure theory
θ	angle between C and magnetic field H
λ	spin-orbit splitting energy
μ_B	Bohr magneton

REFERENCES

1. Woollam, John A.: Graphite Carrier Locations and Quantum Transport to 10 T (100 kG). *Phys. Rev.*, vol. 3B, no. 4, Feb. 15, 1971, pp. 1148-1159.
2. Woollam, John A.: Quantum Galvanomagnetic and Thermomagnetic Effects in Graphite to 18 Teslas (180 kG) at Low Temperatures. NASA TN D-7037, 1971.
3. Williamson, S. J.; Foner, S.; and Dresselhaus, M. S.: de Haas-van Alphen Effect in Pyrolytic and Single-Crystal Graphite. *Phys. Rev.*, vol. 140, no. 4A, Nov. 15, 1965, pp. 1429-1447.
4. Galt, J. K.; Yager, W. A.; and Dail, H. W., Jr.: Cyclotron Resonance in Graphite. *Phys. Rev.*, vol. 103, no. 5, Sept. 1, 1956, pp. 1586-1587.
5. Lax, Benjamin; and Zeiger, H. J.: Possible Interpretation of Cyclotron Resonance Absorption in Graphite. *Phys. Rev.*, vol. 105, no. 5, Mar. 1, 1957, pp. 1466-1468.
6. Soule, D. E.: Magnetic Field Dependence of the Hall Effect and Magnetoresistance in Graphite Single Crystals. *Phys. Rev.*, vol. 112, no. 3, Nov. 1, 1958, pp. 698-707.
7. McClure, J. W.: Analysis of Multicarrier Galvanomagnetic Data for Graphite. *Phys. Rev.*, vol. 112, no. 3, Nov. 1, 1958, pp. 715-721.
8. Soule, D. E.: Change in Fermi Surfaces of Graphite by Dilute Acceptor Doping. *IBM J. Res. Develop.*, vol. 8, no. 3, July 1964, pp. 268-273.
9. Anderson, J. R.; O'Sullivan, W. J.; Schirber, J. E.; and Soule, D. E.: Effect of Pressure on the Fermi Surface of Graphite. *Phys. Rev.*, vol. 164, no. 3, Dec. 15, 1967, pp. 1038-1042.
10. Flood, D. J.: Magnetothermal Oscillations in Pressure-Annealed Pyrolytic Graphite. *Phys. Letters*, vol. 30A, no. 3, Oct. 6, 1969, pp. 178-179.
11. Flood, Dennis J.: Magnetothermal Oscillations in Pressure-Annealed, Pyrolytic Graphite. NASA TN D-5488, 1969.
12. Woollam, John A.: Spin Splitting, Fermi Energy Changes, and Anomalous g Shifts in Single-Crystal and Pyrolytic Graphite. *Phys. Rev. Letters*, vol. 25, no. 12, Sept. 1970, pp. 810-813.
13. Spain, I. L.; Ubbelohde, A. R.; and Young, D. A.: Electronic Properties of Well Oriented Graphite. *Phil. Trans. Roy. Soc. (London)*, Ser. A, vol. 262, no. 1128, Oct. 6, 1967, pp. 345-386.

14. Shoenberg, D.: The de Haas-van Alphen Effect. Progress in Low Temperature Physics. Vol. 2. C. J. Gorter, ed., North-Holland Publ. Co., 1957, p. 226.
15. Argyres, Petros N.: Quantum Theory of Transport in a Magnetic Field. Phys. Rev., vol. 117, no. 2, Jan. 15, 1960, pp. 315-328.
16. Slonczewski, J. C.; and Weiss, P. R.: Band Structure of Graphite. Phys. Rev., vol. 109, no. 2, Jan. 15, 1958, pp. 272-279.
17. McClure, J. W.: Band Structure of Graphite and de Haas-van Alphen Effect. Phys. Rev., vol. 108, no. 3, Nov. 1, 1957, pp. 612-618.
18. Schroeder, P. R.; Dresselhaus, M. S.; and Javan, A.: High-Resolution Magneto-spectroscopy of Graphite. Presented at the American Physical Society Conference on the Physics of Semimetals and Narrow Gap Semiconductors, Dallas, Texas, Mar. 20-21, 1970.
19. Nozières, Philippe: Cyclotron Resonance in Graphite. Phys. Rev., vol. 109, no. 5, Mar. 1, 1958, pp. 1510-1521.
20. Soule, D. E.; McClure, J. W.; and Smith, L. B.: Study of the Shubnikov-de Haas Effect. Determination of the Fermi Surfaces of Graphite. Phys. Rev., vol. 134, no. 2A, Apr. 20, 1964, pp. 453-470.
21. McClure, J. W.; and Yafet, Y.: Theory of the g-Factor of the Current Carriers in Graphite Single Crystals. Proceedings of the Fifth Conference on Carbon. Pergamon Press, 1962, p. 22.
22. Woollam, John A.: Spin Splitting of Graphite Landau Levels, and Fermi Energy Changes with Magnetic Field. Bull. Am. Phys. Soc., vol. 16, no. 1, Jan. 1971, p. 63.

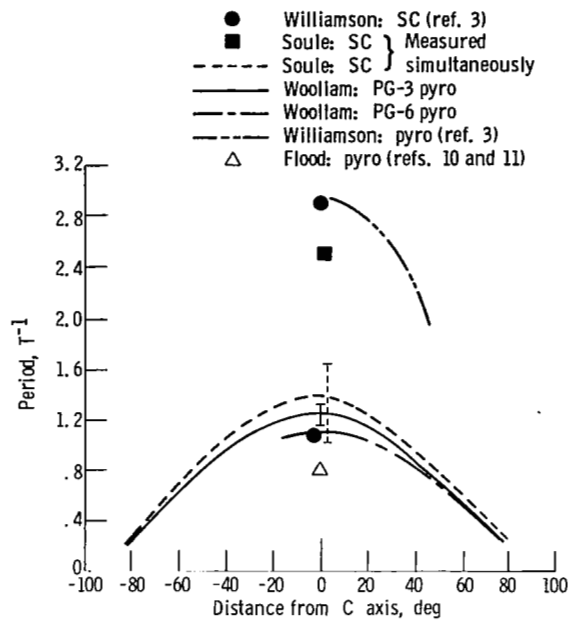


Figure 1. - de Haas - van Alphen periods as function of angle between magnetic field and C axis. Some error bars omitted for clarity. Figure summarizes data on four pyrolytic and two natural single-crystal samples. Single crystal, SC; pyrolytic graphite, PG pyro.

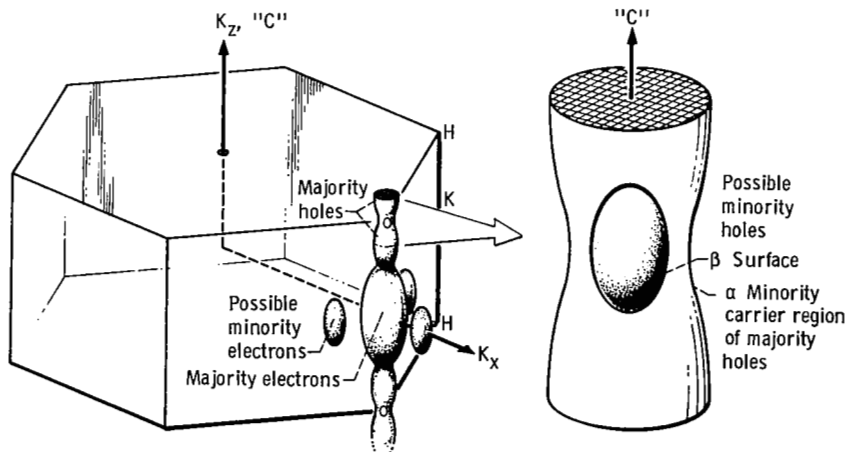


Figure 2. - Majority, and possible minority carrier Fermi surfaces of graphite and Brillouin zone. Identical Fermi surfaces, located along the five other Brillouin zone edges are omitted for clarity.

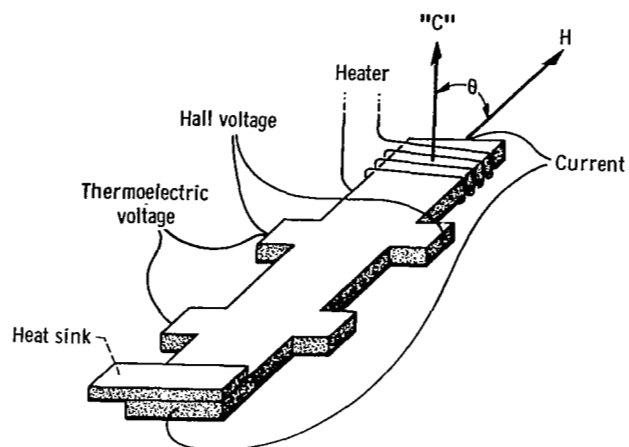


Figure 3. - Sample geometry for Hall effect and thermopower measurements.

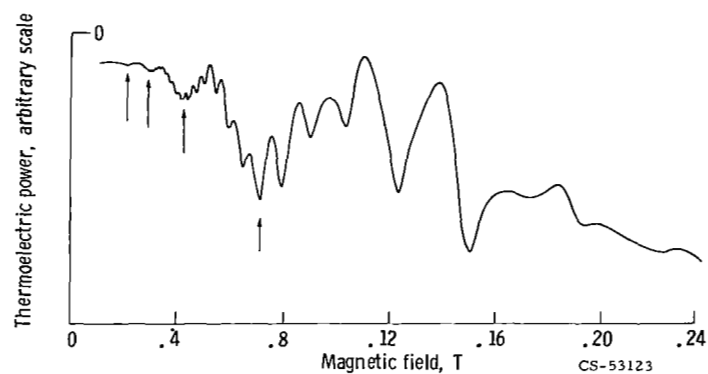


Figure 4. - Thermoelectric power as function of magnetic field ($I_t = 10$ kG) at 1.2 K in PG-3. Minority extrema marked by arrows; magnetic field 10° from C axis.

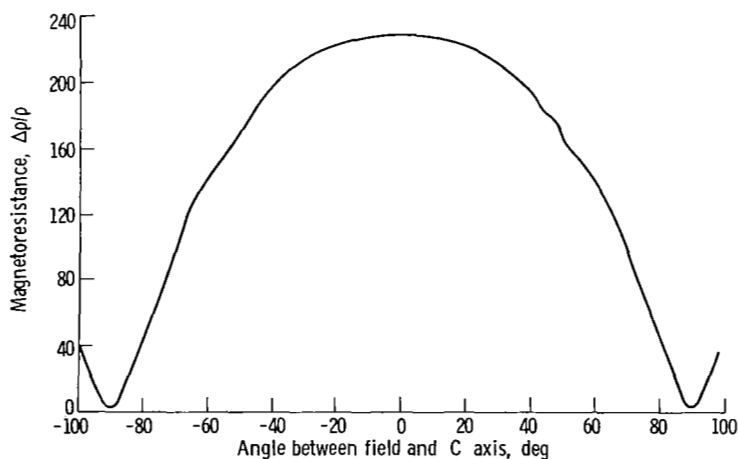


Figure 5. - Magnetoresistance as function of angle between field and C axis. Plot used to locate accurately perpendicularity to C axis; magnetoresistance of PG-6, 10.2 teslas.

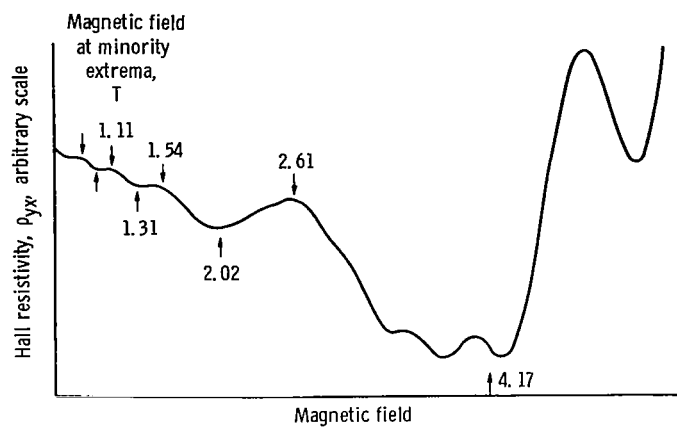


Figure 6. - Hall resistivity ρ_{yx} as function of magnetic field at 1.1 K with magnetic field 77° from C axis. PG-6 pyrolytic graphite; magnetic field 77° from C axis.

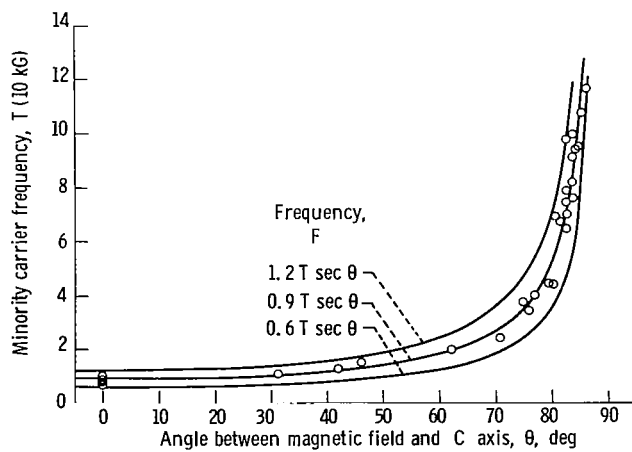


Figure 7. - Quantum oscillation frequency as function of angle between magnetic field and C axis for PG-6.

NATIONAL AERONAUTICS AND SPACE ADMINISTRATION
WASHINGTON, D. C. 20546

OFFICIAL BUSINESS
PENALTY FOR PRIVATE USE \$300

FIRST CLASS MAIL



POSTAGE AND FEES PAID
NATIONAL AERONAUTICS AND
SPACE ADMINISTRATION

014 001 C1 U 26 710813 S00903DS
DEPT OF THE AIR FORCE
AF SYSTEMS COMMAND
AF WEAPONS LAB (WLOL)
ATTN: E LOU BOWMAN, CHIEF TECH LIBRARY
KIRTLAND AFB NM 87117

POSTMASTER: If Undeliverable (Section 158
Postal Manual) Do Not Return

"The aeronautical and space activities of the United States shall be conducted so as to contribute . . . to the expansion of human knowledge of phenomena in the atmosphere and space. The Administration shall provide for the widest practicable and appropriate dissemination of information concerning its activities and the results thereof."

—NATIONAL AERONAUTICS AND SPACE ACT OF 1958

NASA SCIENTIFIC AND TECHNICAL PUBLICATIONS

TECHNICAL REPORTS: Scientific and technical information considered important, complete, and a lasting contribution to existing knowledge.

TECHNICAL NOTES: Information less broad in scope but nevertheless of importance as a contribution to existing knowledge.

TECHNICAL MEMORANDUMS: Information receiving limited distribution because of preliminary data, security classification, or other reasons.

CONTRACTOR REPORTS: Scientific and technical information generated under a NASA contract or grant and considered an important contribution to existing knowledge.

TECHNICAL TRANSLATIONS: Information published in a foreign language considered to merit NASA distribution in English.

SPECIAL PUBLICATIONS: Information derived from or of value to NASA activities. Publications include conference proceedings, monographs, data compilations, handbooks, sourcebooks, and special bibliographies.

TECHNOLOGY UTILIZATION PUBLICATIONS: Information on technology used by NASA that may be of particular interest in commercial and other non-aerospace applications. Publications include Tech Briefs, Technology Utilization Reports and Technology Surveys.

Details on the availability of these publications may be obtained from:

SCIENTIFIC AND TECHNICAL INFORMATION OFFICE
NATIONAL AERONAUTICS AND SPACE ADMINISTRATION
Washington, D.C. 20546